Trieste – June 11-14 2024

Geophysical evidence for gas hydrate/free gas associated with mud volcanism in the western Ross Sea (Antarctica)

Riccardo Geletti[1], Martina Busetti[1], Giuseppe Brancatelli[1], Dario Civile[1], Chiara Sauli[1], Edy Forlin[1], Vincenzo Lipari[1]

[1] *National Institute of Oceanography and Applied Geophysics - OGS, Trieste (Italy), rgeletti@ogs.it*

Geophysical evidence of gas hydrates associated with mud volcanism has been found in the western Ross Sea (Geletti & Busetti, 2011, 2022; Busetti et al., 2024). The location of the mud volcanoes (Fig. 1) appears to be closely related to the tectonic structures in this area (Sauli et al., 2021) and the fluid releases, with the zone where Bottom Simulating Reflectors (BSRs) are strongly pronounced in the seismic profiles (Figs. 2, 4, 5, 6). These BSRs describe the transition between gas hydrate and free gas. The presence of the reservoir appears to be associated with morpho-structural high zones that may act as traps for the gas, which is present in both the solid and gaseous phases. Mud volcanism is generally involving voluminous generation and emission of methane and carbon dioxide, which means that most mud volcanoes serve as an efficient, natural source of greenhouse gasses and consequently play an important role in global climate dynamics (Judd, 2005). The system of mud volcanoes and gas-bearing sediments in the western Ross Sea (Figs. 2 and 3) could therefore be a source of methane flux from the lithosphere to the hydrosphere and atmosphere, as recent studies along the coastal margin have also shown (Seabrook et al., 2023), and thus impact on the greenhouse effect and climate change.

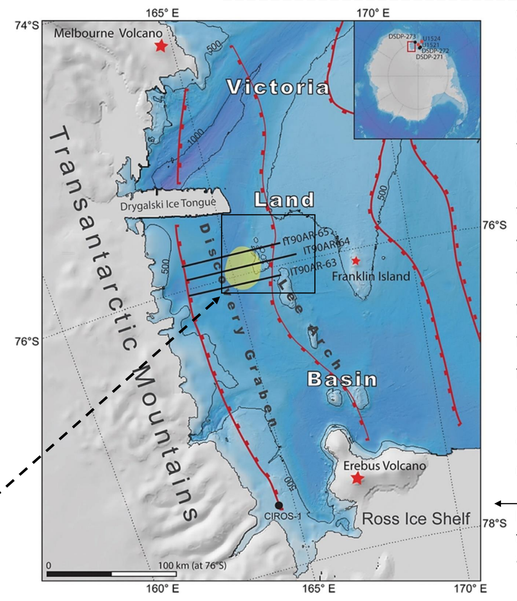

Map of the western Ross Sea with the position of the analysed multi-channel seismic profiles and the area (yellow) with the occurrence of the bottom simulating reflectors (Geletti & Busetti, 2022). Red stars indicate recent volcanoes, red lines are the boundaries of the sedimentary basins.

We present a reprocessing of multichannel seismic profiles that provides evidence for a plumbing system feeding the mud volcanoes, with gas leaking from the seafloor in the western Ross Sea (Geletti and Busetti, 2011, 2022; Geletti et al., 2017; Busetti et al., 2024). In pre-stack analysis (Figs. 7 and 8), BSRs in the seismic records are characterized by several anomalies in amplitude, velocity and frequency compared to the normal adjacent seismo-stratigraphic reflectors (Geletti & Busetti, 2011, 2022): (a) the amplitude of the reflection varies with offset, with its negative value increasing with distance (or incidence angle) and absolute values comparable to those of the seafloor reflection; (b) the velocity function at the level of the BSR decreases drastically, going from about 2000 m/s to less than 1400 m/s in the underlying layer; (c) the dominant frequency of the BSR is below 25 Hz of the seismostratigraphic reflectors at the same time twt (Fig. 6b$_2$). On the stacking profiles, the BSRs appear with events of strongly negative amplitude, simulating the trend of seafloor deepening with increasing bathymetric depth, cutting the horizons in some areas regardless of stratigraphy. These BSRs are discontinuous and are interrupted near some active faults in the Lee Arch (acoustic gap), at the top of which morpho-bathymetric reliefs and depressions such as mud volcanoes and pockmarks can be recognized.

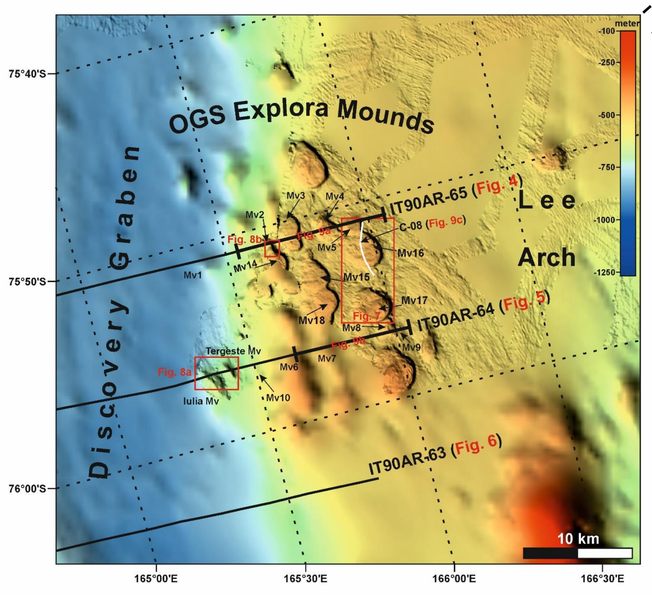

Figure 1 - Morpho-bathymetric map of study area (modified from Busetti et al., 2024), named OGS Explora Mounds in 2007 (SCAR Composite Gazetteer of Antarctica https://data.aad.gov.au/aadc/gaz/scar), showing the morphologies and distribution of mud volcanoes (Mv) on the structural high of Lee Arch. The morpho-bathymetric map was produced by merging the low resolution data from the IBCSO with the high resolution data acquired by OGS in 2006 and USGS data (http://www.marine-geo.org). The black and white lines indicate the multichannel seismic and chirp profiles used in this study, respectively.

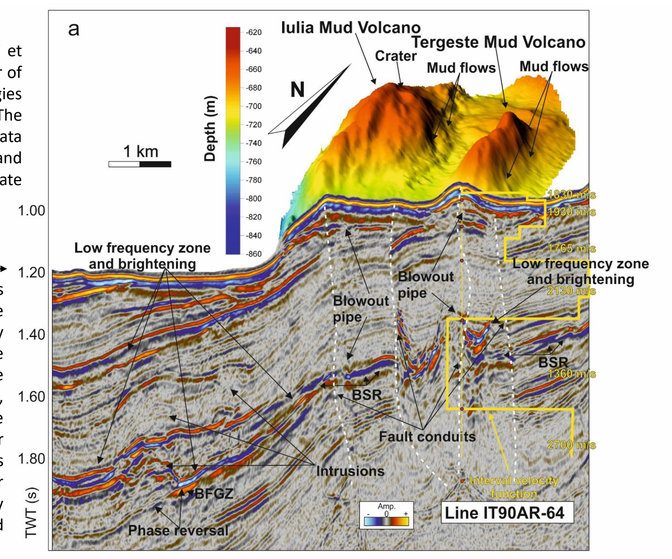

Figure 2 - The Iulia and Tergeste mud volcanoes and associated gas plumbing system in the eastern sector of the Discovery Graben (see Fig. 1 for location): a) morpho-bathymetric data evidence the roughly north-south elongate shape of the mud volcanoes, which are associated with faults: Tergeste consists of three main cones, while Iulia consists of a ridge with a main central body with a crater on top, both MVs being draped with mudflows on the flanks. Part of the multi-channel seismic profile IT90AR-64 (see Fig. 5), modified after Geletti and Busetti (2011, 2022), shows acoustic evidence of gas occurrence and migration such as the Bottom Simulating Reflector (BSR), the Base of the Free Gas Zone (BFGZ), the Low Frequency Zone and brightening disturbed horizons near fault conduits and blowout pipes indicating fluid migration feeding the mud volcanoes; b) reflection strength section shows the high amplitude zone beneath the mud volcanoes associated with the gas reservoir, as also shown in c) by the instantaneous frequency section with the low frequency zones.

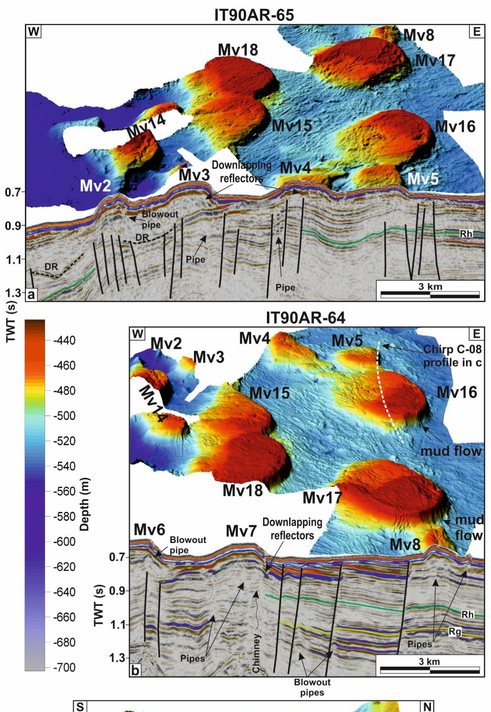

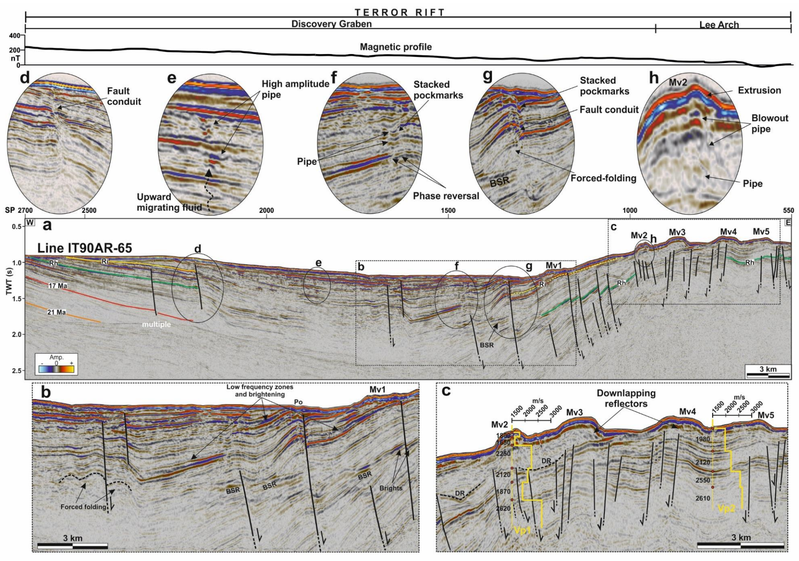

Figure 4 - Multichannel seismic line IT90AR-65 (see Fig. 1 for location), showing the occurrence of mud volcanoes (Mv) up to 1.5 km wide, lying on the Late Miocene erosive sea floor surface of Lee Arch.

The seismic profile evidenced features related to fluid occurrence and migration: the Bottom Simulating Reflector (BSR) as the interface between gas hydrate above and free gas below (Figs. 4a, b, g); the Downdipping Reflector (DR) at the base of the Mv2 and Mv3, that represents an abrupt change of the interval velocities from 2250 m/s above to 1870 m/s below in Vp1, suggesting gas occurrence feeding the mud volcanoes, unlike the Vp2 with a normal velocity increment outside (Fig. 4c); fluid migration along fault conduits (Fig. 4d, g), high amplitude pipe (Fig. 4e) and blowout pipe feeding the mud volcano Mv2 (Fig. 4h); forced-folding due to fluid and mud intrusion (Fig. 4b, g); stacked pockmarks related fluids expulsion (Fig. 4g); low frequency zone, brightening (Fig. 4b) and phase reversal (Fig. 4f) related to gas bearing sediment. The magnetic profile at the top of the figure does not show any significant anomalies at the mud volcanoes.

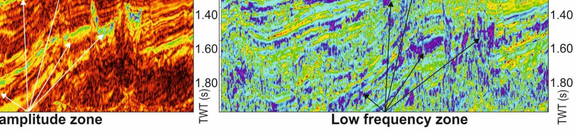

Figure 5 - Multichannel seismic line IT90AR-64 (see Fig. 1 for location), showing the occurrence of mud volcanoes (Mv) up to 2 km wide, lying on the Late Miocene erosional sea floor surface of Lee Arch. Iulia and Tergeste mud volcanoes (SCAR Composite Gazetteer of Antarctica, https://data.aad.gov.au/aadc/gaz/scar) were identified by Geletti and Busetti (2011; 2022). The seismic profile shows evidence of features related to gas/fluid occurrence and migration: the Bottom Simulating Reflector (BSR) as the interface between gas hydrate above and free gas below interrupted by a wide bright zone chimney (about 500 m) (Fig. 5a, d); wipe out zone with disrupted reflectors (Fig. 5a); pipes and blowout pipes associated with upward migration of gas/fluid and feeding the mud volcanoes (Fig. 5b, f); fault conduits with brightening horizons due to gas occurrence (Fig. 5e); forced-folding associated with fluid/mud intrusion with onlap of the above horizons (Fig. 5c). Velocity profile Vp1 through the Mv8 shows velocity inversion below the base of the Mv from 1990 m/s to 1590 m/s indicating gas bearing sediment below; the velocity profile Vp2 through the sedimentary sequence shows no abrupt inversion (Fig. 5b). The magnetic profile in the upper part of the figure, shows no significant anomalies in correspondence of the mud volcanoes.

Figure 6 - Multichannel seismic line IT90AR-63 (see Fig. 1 for location), shows evidence of features related to gas/fluid occurrence and migration: small mud volcanoes (Mv10, 11 and 12) lying at the border of a 2 km wide diatreme crater with the ejecta ring and the underlying V-shape conduit (Fig. 6a, c); the Bottom Simulating Reflector (BSR) as the interface between gas hydrate above and free gas below (Fig. 6a, b) interrupted by a nearly 1 km wide chimney marked by a bright zone associated with gas occurrence, and feeding the Mv13 (Figs. 6b and 6b$_1$); fault conduits below a pockmark (Fig. 6d); buried pockmarks near the giant pockmark (Fig. 6c); wipe out zone and low frequency zone associated with the gas presence (Figs. 6a, c). The magnetic profile show no significant anomalies. The low frequency (inside the black circle in (b$_2$)—the frequency spectrum vs TWT panel) is an indicator of the free-gas occurrence (Geletti & Busetti, 2011, 2022).

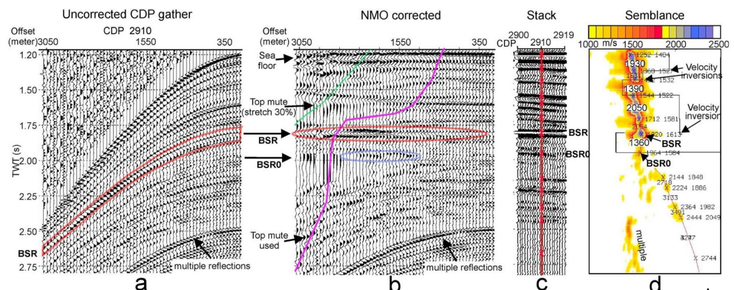

Fig. 7: Image of a common depth point (CDP) from the IT90AR-63 profile in Fig. 6b$_1$, showing a double BSR (Geletti & Busetti, 2011): (a) 60-fold CDP 2910 gather after AGC and (b) after normal moveout correction (NMO) showing the strongest BSR; (c) stack section on 20 CDP around CDP 2910; and (d) semblance velocity analysis and its relation to the BSR/BSR0 pair.

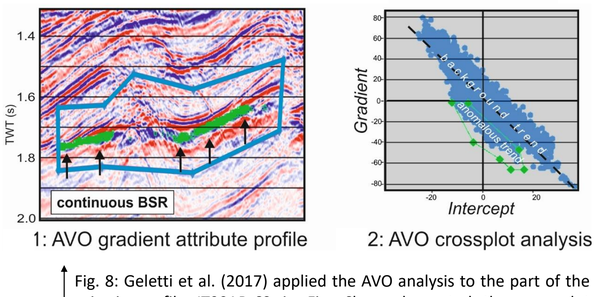

Fig. 8: Geletti et al. (2017) applied the AVO analysis to the part of the seismic profile IT90AR-63 in Fig. 6b$_1$ and created the cross-plot between the AVO attribute gradient and the intercept to check the lithological variation. The authors note that the general trend of sedimentation in the blue polygon in Fig. 8$_1$ is characterised by the background trend passing through the origin of the axis (Fig. 8$_2$). A group of points lies outside this trend (green polygon in Fig. 8$_2$) and is displaced from the origin of the axis towards the lower left quadrant. If we enclose these points in a green polygon, we find that they correspond to the values of gradient and intercept representing the BSR and its lower part in the AVO gradient attribute section in Fig. 8$_1$.

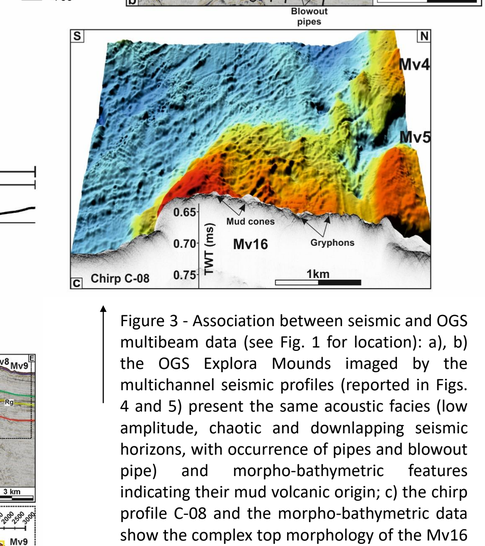

Figure 3 - Association between seismic and OGS multibeam data (see Fig. 1 for location): a), b) the OGS Explora Mounds imaged by the multichannel seismic profiles (reported in Figs. 4 and 5) present the same acoustic facies (low amplitude, chaotic and downlapping seismic horizons, with occurrence of pipes and blowout pipe) and morpho-bathymetric features indicating their mud volcanic origin; c) the chirp profile C-08 and the morpho-bathymetric data show the complex top morphology of the Mv16 associated with the presence of mud cones and gryphons.

AVO crossplot analysis area

Anomalous trend zone in the AVO IG crossplot diagram

References

- Busetti, M., Geletti, R., Civile, D., Sauli C., Brancatelli G., Forlin E., et al. (2024). Geophysical evidence of a large occurrence of mud volcanoes associated with gas plumbing system in the Ross Sea (Antarctica). *Geoscience Frontiers*, 2024, 15(1), 101727. https://doi.org/10.1016/j.gsf.2023.101727
- Geletti, R., & Busetti, M., (2022). *Bottom Simulating Reflector in the western Ross Sea, Antarctica*. In: Mienert, J., et al., (Eds), World Atlas of Submarine Gas Hydrate in Continental Margins, 475-482. https://doi.org/10.1007/978-3-030-81186-0_40
- Geletti, R., Mocnik, A., Busetti, M., Civile, D., Del Ben, A., (2017). Different origins of BSRs in Antartic sedimentary environments. Past Antarctic Ice Sheet Dynamics (PAIS) Conference, September 10-15th 2017, Trieste – Italy.
- Geletti, R., & Busetti, M. (2011). A double bottom simulating reflector in the western Ross Sea, Antarctica. *Journal of Geophysical Research*, 116, B04101, https://doi.org/10.1029/2010JB007864
- Judd, A. (2005). *Gas emissions from mud volcanoes. Significance to Global Climate Change*. In Martinelli G., Panahi B., (ed.) Mud Volcanoes, Geodynamics and Seismicity, 51(4), 147-157.
- Sauli, C., Sorlien, C., Busetti, M., De Santis, L., Geletti, R., Wardell, N., Luyendyk, B.P., (2021). Neogene development of the Terror Rift, western Ross Sea, Antarctica. *Geoch., Geoph., Geos.* 22/3, 1-20. https://doi.org/10.1029/2020GC009076
- Seabrook, S., Law, C., Thurber, A., Ladroit, Y., Cummings, V., Tait, L., et al. (2023). Emergent Antarctic seafloor seeps: A tipping point reached? Preprint, *Nature portfolio*. https://doi.org/10.21203/rs.3.rs-3657723/v1